HOSTED BY

ELSEVIER

Available online at www.sciencedirect.com

ScienceDirect

Journal of Magnesium and Alloys 4 (2016) 173–180
www.elsevier.com/journals/journal-of-magnesium-and-alloys/2213-9567

Full Length Article

Unexpected formation of hydrides in heavy rare earth containing magnesium alloys

Yuanding Huang [a,*], Lei Yang [a,b], Sihang You [a], Weimin Gan [a], Karl Ulrich Kainer [a], Norbert Hort [a]

[a] *Institute of Materials Research, Helmholtz-Zentrum Geesthacht, Zentrum für Material- und Küstenforschung, Max-Planck-Str. 1, 21502 Geesthacht, Germany*
[b] *Key Laboratory for Anisotropy and Texture of Materials, Education Ministry of China, School of Materials Science and Engineering, Northeastern University, Shenyang 110819, China*

Received 7 July 2016; revised 16 August 2016; accepted 21 August 2016

Available online 31 August 2016

Abstract

Mg–RE (Dy, Gd, Y) alloys show promising for being developed as biodegradable medical applications. It is found that the hydride REH_2 could be formed on the surface of samples during their preparations with water cleaning. The amount of formed hydrides in Mg–RE alloys is affected by the content of RE and heat treatments. It increases with the increment of RE content. On the surface of the alloy with T4 treatment the amount of formed hydride REH_2 is higher. In contrast, the amount of REH_2 is lower on the surfaces of as-cast and T6-treated alloys. Their formation mechanism is attributed to the surface reaction of Mg–RE alloys with water. The part of RE in solid solution in Mg matrix plays an important role in influencing the formation of hydrides.

Keywords: Magnesium alloy; Microstructure; Hydride; Heat treatment; Rare earths

1. Introduction

The applications of magnesium alloys are being extended as they are not only developed as structural materials for transportation industrial applications, but also as biodegradable implant materials for medical applications. In order to improve the performance of previous magnesium alloys or further to develop new magnesium alloys, rare earths (REs) are popularly selected as alloying elements to add to magnesium. Several advantages are found when REs are added to magnesium, including the improvement of both the room and high temperature mechanical properties [1]. One typical example is the development of heat resistant AE42 and AE44 alloys. The addition of mischmetal in Mg–Al results in the formation of thermal stable Al–RE intermetallics, which effectively supply the resistance to grain boundary sliding at high temperatures, and consequently increase the creep fatigue life. Compared with non-RE (Rare Earths) containing magnesium alloys, the RE-containing alloys have a better corrosion resistance [2,3]. Luo's results show that the addition of 0.2% Y to AZ91 alloy increases its corrosion resistance by 7 times [4]. Owing to their suitable mechanical properties and acceptable corrosion resistance, Mg–RE alloys were recently regarded as one of the most potential degradable biomaterials [5–9].

High reactivity of rare earths (such as Y, La, Ce, Pr, Nd, Gd, Tb, Dy, and Er) with H_2 and H_2O to form dihydride or hydroxide is well known even at room temperature [10]. From their preparations to final applications RE containing magnesium alloys are inevitably exposed to the environment containing hydrogen (H). Due to the fact that REs have a high chemical activity, it is of particular interest to investigate the possible interactions between RE and H in Mg–RE alloys. Recently, besides the RE-containing second phases, a cuboid RE-dominated phase was often observed in Mg–RE alloys which is not presented in Mg–RE phase diagrams. Yang et al. reported that NdH_2 was formed in Mg–2wt.%Nd alloy with T4 treatment [11]. The formation of NdH_2 was attributed to the reaction of Nd with the previously dissolved hydrogen during casting. Another different explanation was given by Peng et al. [12]. It is suggested that the formation of hydride in Mg–Gd alloys can also proceed during sample preparations or even mechanical deformation if subjected to H-containing environment. The hydride could be formed even at room temperature by interacting with the external

* Corresponding author. Institute of Materials Research, Helmholtz-Zentrum Geesthacht, Zentrum für Material- und Küstenforschung, Max-Planck-Str. 1, 21502 Geesthacht, Germany. Fax: +49 4152 871909.
E-mail address: yuanding.huang@hzg.de (Y. Huang).

http://dx.doi.org/10.1016/j.jma.2016.08.002

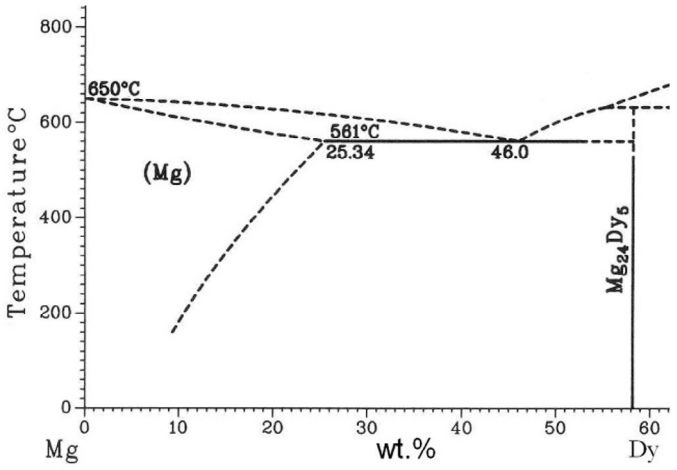

Fig. 1. Mg rich side of binary Mg–Dy phase diagram [14].

H-agents such as water vapour in air or water. Recently, Zhu et al. investigated the unexpected formation of hydride for the as-cast Mg–RE (La, Ce, Nd) alloys. They suggested that the formation of hydride was not attributed to these two mechanisms. They proposed that the formation of hydride is related to the decomposition of Mg–RE intermetallics by hydrogen during solidification or high temperature heat treatment [13]. In summary, at present the responsible mechanisms for the unexpected formation of hydride are still argued. Further investigations are necessary.

The present work will investigate the influences of alloying element REs and heat treatments on the formation of hydrides in Mg–RE alloy. The formation mechanism will be clarified, including where the H-agent comes from. REs as alloying elements in Mg include two groups: light REs such as La, Ce, Nd, Pr etc. and heavy REs such as Y, Gd, Dy, Sm etc. REs in each group have similar physical and chemical properties. These heavy REs including Y, Gd and Dy in magnesium are focused in the present work, which have normally a large solid solubility in Mg (Fig. 1) [14]. As aforementioned, the possible formation of hydride in light heavy REs (including La, Ce, Nd) containing magnesium alloy has been investigated by Zhu et al. [13]. Heavy RE containing magnesium alloys have potential applications as degradable biomaterials. During their degradation, the gas hydrogen is released. The present investigation is helpful for understanding the degradation process in the body environment with water and how about the interactions between the REs and hydrogen ions during degradation process (for example, suppression of hydrogen gas release). In addition, when these alloys are used as structural components in the moisture atmospheres, likewise, the interactions between the water and these alloys could happen. Thus, the present investigation is also beneficial for exploring and understanding such interactions in the moisture environment.

2. Experimental procedures

High-purity Mg was molten in a mild steel crucible under a protective atmosphere (Ar + 2% SF_6). Pure Y, Gd, and Dy were added at a melt temperature of 720 °C to prepare binary Mg–Y, Mg–Gd and Mg–Dy alloys. The melt was stirred at 200 rpm for 30 min. After that, the melt was cast with directly chilled permanent mould casting method. The melt was poured into a mould preheated at 500 °C. The filled mould was held at 670 °C for 30 min under protective gas. Then the whole steel crucible with the melt was immersed into the continuous cooling water at a rate of 10 mm/s. When the bottom of steel crucible touched the water, it was stopped for 1 second. As soon as the liquid level of inside melt was in alignment with the height of outside water level [15], the solidification process was finished. The size of ingot is 6 cm × 12 cm × 20 cm. Solution treatment (T4 treatment) was done under 520 °C for 24 h followed by water quenching. The ageing treatment was carried out at 250 °C for 16 h followed by air cooling.

The hydrogenation treatment was carried out at 520 °C under an atmosphere of Ar plus 5% H_2 with a pressure of 1.013×10^{-3} Pa, and treatment time was one hour. After hydrogenation treatment, the samples were furnace cooled to room temperature.

Samples for microstructural observations were prepared in two ways:

(1) After cutting, the specimens were ground and mechanically polished with water (termed preparation process No. 1).
(2) After cutting, the samples were ground and mechanically polished with organic solvent such as high pure ethanol, instead of water. After the specimens were further electropolished, they were performed with microstructural observations as soon as possible (termed preparation process No. 2).

After the samples were grinded and polished, they were cleaned with water, then with alcohol and finally dried. The dried samples were observed in SEM immediately or soon, if cannot, they were stored in a low vacuum environment. Microstructures were investigated using a Zeiss Ultra 55 (Carl Zeiss GmbH, Oberkochen, Germany) scanning electron microscopy (SEM) equipped with energy dispersive X-ray analysis (EDX). Specimens for transmission electron microscopy (TEM) were ground mechanically to about 120 μm with the assistance of water and then thinned by electropolishing in a twin jet system using a solution of 2.5% $HClO_4$ and 97.5% ethanol at about −45 °C and a voltage of 40 V. Moreover, TEM sample was also prepared by 30 keV Ga^+ focused ion beam (FIB) technology to identify the hydride clearly. The TEM examinations were carried out on a Philips CM 200 instrument with an energy dispersive X-ray analysis (EDX) system operating at 200 kV. X-ray diffraction (XRD) investigations were also carried out using a Siemens diffractometer operating at 40 kV and 40 mA with Cu k_α radiation. Measurements were obtained by step scanning 2Θ from 20 to 90° with a step size of 0.02°. A count time of 3 seconds per step was used.

3. Results

Mg–Y, Mg–Gd and Mg–Dy systems have a similar phase diagram and belong to eutectic system (Fig. 1). Their solidification

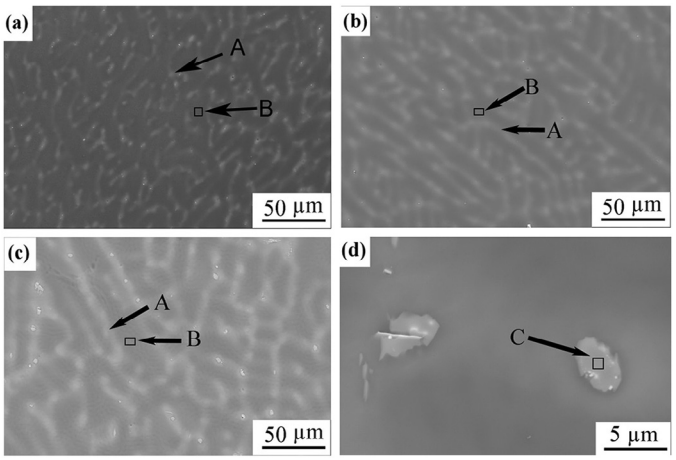

Fig. 2. SEM microstructures of the as-cast Mg–Dy alloys: (a) Mg–10Dy; (b) Mg–15Dy; (c) Mg–20Dy; (d) High magnification of second phase in Mg–20Dy alloy. (Arrow A: segregation of Dy; Arrow B: Mg matrix; Arrow C: second phase).

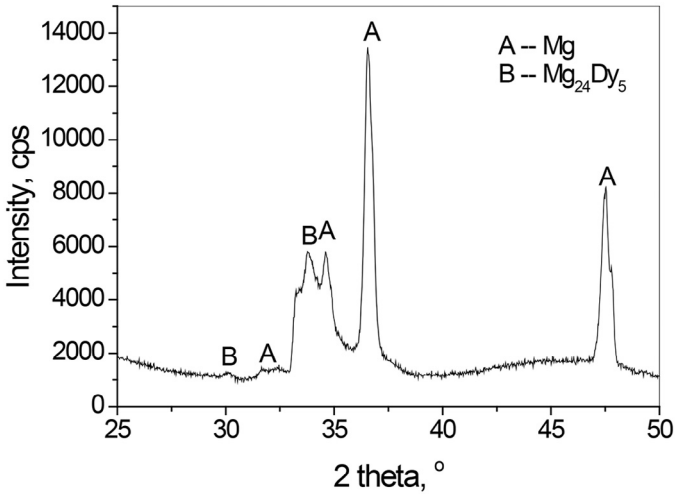

Fig. 3. XRD pattern of the as-cast Mg–20Dy alloy.

microstructures are not so much different. The following sessions will take Mg–Dy system as an example to show the related results. Some other results such as microstructural observations and second phase identification can also be found in the previous publications [12,16].

3.1. Microstructural observations of Mg–Dy alloys

As shown in Mg–Dy binary phase diagram (Fig. 1), only one second phase $Mg_{24}Dy_5$ exists when the content of Dy is below 60 wt.%. Fig. 2 shows the SEM observations on the microstructures of Mg–Dy binary alloys. Their microstructures are characterized with the dendrites with the alloying element Dy enriched at the dendritic boundaries. The content of Dy in Mg matrix (as indicated by arrow B) is about half its designed content. For example, the content of Dy in Mg matrix is 10.3 wt.% for Mg–20Dy alloys. The content of Dy in the segregation area (as indicated by arrow A) is much higher than that in the matrix. It increases gradually with the increment of Dy content. It increases from 21.7 to 29.2 wt.% when the content of added Dy increases from 10 to 20 wt.%. EDX analysis demonstrates that the composition of second phase (Fig. 2(d)) is about 85% Mg, 14% Dy and 1% O in atomic percent. Based on the measured atomic ratio of Mg/Dy in this phase and phase situation shown in Mg–Dy binary phase diagram [14], this phase can be concluded as $Mg_{24}Dy_5$ phase. This conclusion is further confirmed by XRD analysis (Fig. 3). Fig. 4 shows the TEM picture of second phase and its corresponding diffraction pattern along zone axis [111]. The diffraction pattern is also consistent with that of stable $Mg_{24}Y_5$ phase in Mg–Y alloy [14]. The crystal structure of phase $Mg_{24}Dy_5$ is the same as that of Mg_5Gd.

3.2. Formation of DyH_2

Fig. 5 shows the comparison of XRD patterns for the samples of T4-treated Mg–20Dy alloy prepared with and without water. On the surface of the sample ground without water, only Mg phase is identified. However, when the sample was ground with water, besides the matrix phase Mg, the phase DyH_2 is also detected. Microstructural observations further demonstrate that there indeed exists a cuboid phase on the surface of the sample ground with water (Fig. 6(b), (c) and (d)), but no such phase on the sample ground without water (Fig. 6(a)). EDX analysis indicates that these cuboid particles contain a very high content of Dy with a value of about 75.5 at.% (Fig. 6(d)). In Mg–Dy binary phase diagram (Fig. 1), no such a phase with so high amount of Dy can be found. Based on the XRD results and microstructural observations, these cuboid particles should be concluded to be the hydride DyH_2. Identifications of TEM diffraction patterns also illustrate that the cuboid particle is DyH_2 with a zone axis of $[0\bar{3}1]$ (Fig. 7).

3.3. Influences of Dy content

The content of Dy influences the formation of hydride DyH_2. When the alloy contains 10% Dy, the XRD cannot detect the hydride DyH_2 (Fig. 8). Actually, microstructural observations indicate that the hydride DyH_2 is formed on the surface of T4-treated Mg–10Dy alloy when it is mechanically polished with water (Fig. 9(a)). For this alloy the amount of formed DyH_2 is small, therefore, it cannot be detected by XRD. When

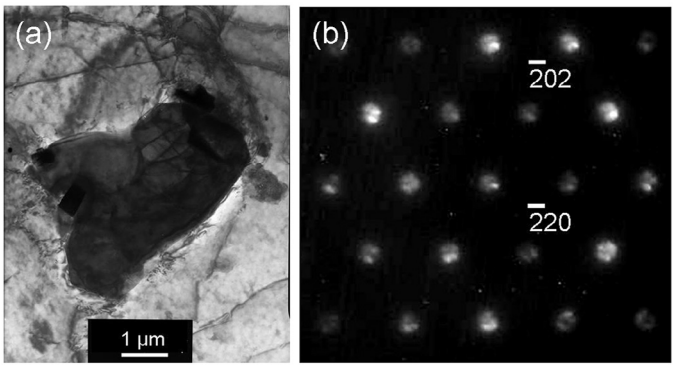

Fig. 4. (a) TEM picture of second phase in the as-cast Mg–20Dy alloy and (b) its corresponding diffraction pattern along zone axis [111].

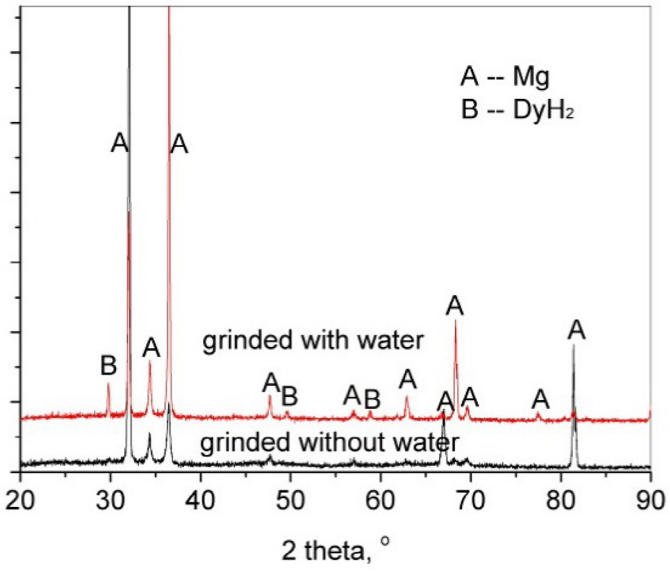

Fig. 5. XRD patterns for the samples of T4-treated Mg–20Dy alloy prepared with and without water.

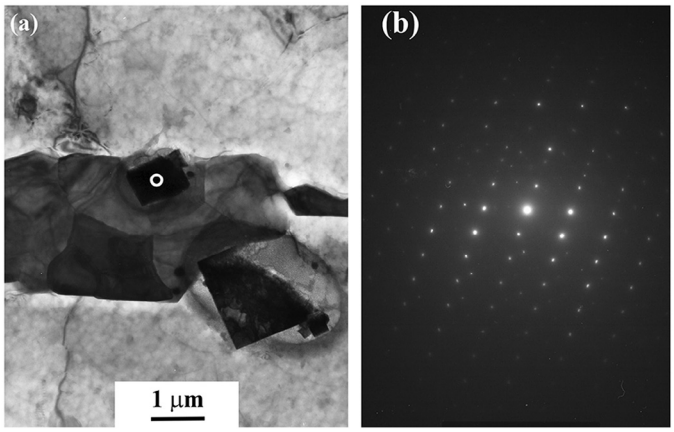

Fig. 7. TEM micrograph showing the hydrides in the as-cast Mg–20Dy alloy: (a) hydride DyH_2 and (b) its corresponding diffraction pattern zone axis = $[0\bar{3}1]$.

the content of Dy increases to 15%, the peaks corresponding to DyH_2 are observed (Fig. 8(a)), indicating that the increment in the content of Dy increases the amount of DyH_2. When the content of Dy further increases to 20%, the intensities of DyH_2 peaks increase a little if compared with that of Mg–15Dy alloy. SEM observations also show that the hydride DyH_2 is formed on the surface of all investigated alloys (Fig. 9). The amount of hydride DyH_2 increases with the increment of Dy content.

3.4. Influences of heat treatments

The formation of hydride DyH_2 was observed on the surface of all Mg–20Dy alloys with different states (Fig. 10). However, XRD results demonstrate that the hydride DyH_2 can only be detected on the surface of Mg–20Dy alloy with T4 treatment (Fig. 8(b)). On the surfaces of as-cast and T6-treated Mg–20Dy alloys, the amount of hydride DyH_2 should be tiny. This is why XRD cannot detect them. On the surface of as-cast Mg–20Dy alloy, the hydride DyH_2 is normally observed at the dendritic boundaries. It locates beside the second phase which was identified as $Mg_{24}Dy_5$ intermetallics (Fig. 10(a)) [17,18]. Its size is about 200–300 nm. After T4 and T6 treatments, the size of DyH_2 increases to about 2–5 μm (Fig. 10(b) and (c)).

4. Discussion

4.1. Formation mechanism of hydrides

The extreme sensitivity of the rare earth metals to H_2 contamination is consistent with previous studies [19–21]. Their

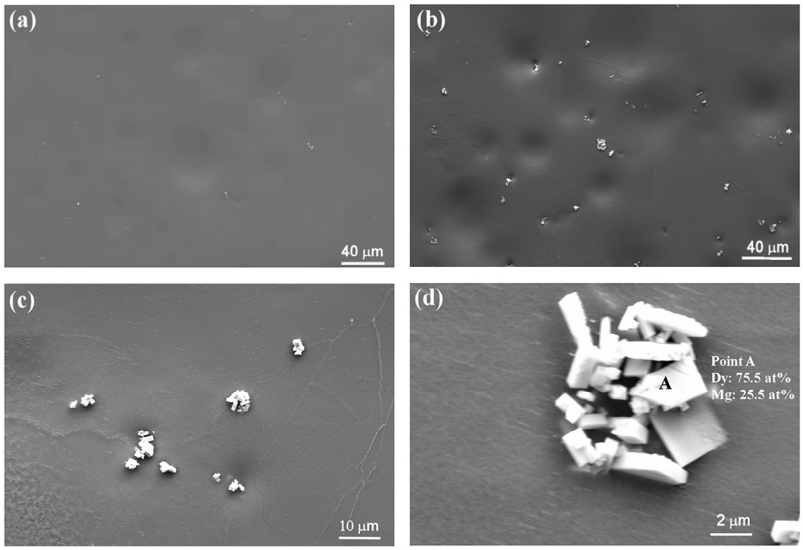

Fig. 6. SEM micrographs showing the surface microstructures of T4-treated Mg–20Dy alloys with different sample preparations: (a) sample preparation No. 2, electropolished without water; (b) sample preparation No. 1, mechanically polished with water; (c and d) sample preparation No. 1, mechanically polished with water, high magnification.

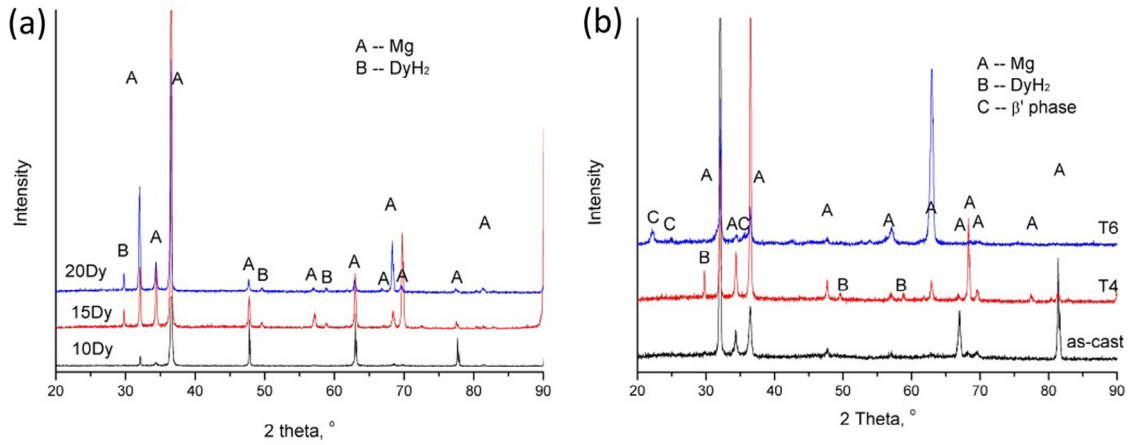

Fig. 8. X-ray diffraction patterns showing the phases: (a) effects of Dy content, Mg–Dy alloys with T4 treatment and (b) effects of heat treatments, Mg–20Dy alloy. The samples were prepared by process No. 1.

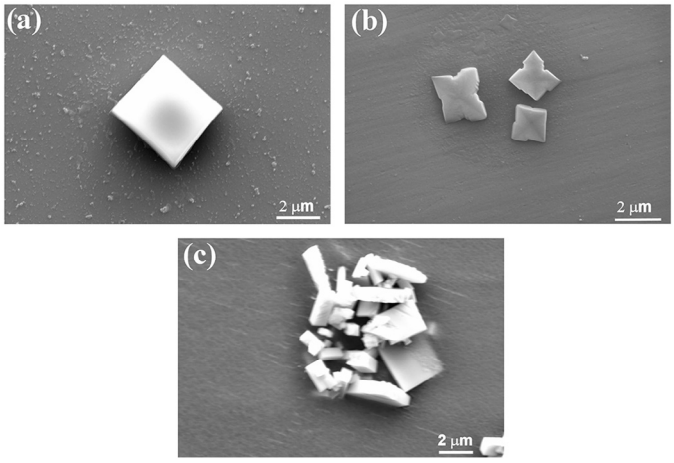

Fig. 9. Formation of hydrides in T4-treated Mg–Dy alloys with different contents of Dy: (a) 10% Dy, (b) 15% Dy and (c) 20% Dy. The samples were prepared by process No. 1.

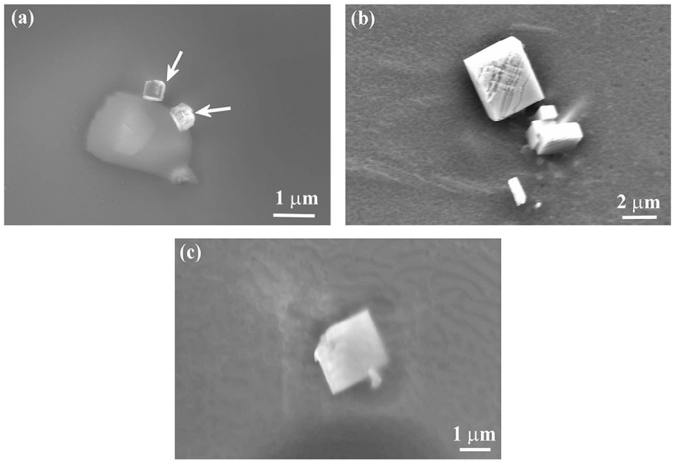

Fig. 10. Formation of hydrides DyH_2 in Mg–20Dy alloys with different states: (a) as-cast, (b) T4 treatment and (c) T6 treatment. The samples were prepared by process No. 1.

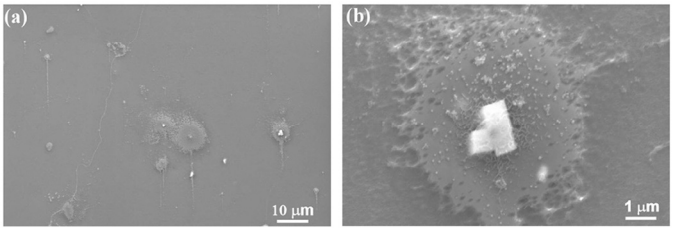

Fig. 11. Formation of hydrides on the surface of Mg–20Dy alloy with T6 treatment: (a) low magnification and (b) high magnification. The samples were prepared by process No. 1.

results indicated that the formation of hydride phases is a common occurrence with rare earth metals and alloys when standard aqueous metallographic techniques or diamond polishing with commercial carrier fluids is employed. The rate of their formation is controlled by bulk diffusion of H.

In order to clarify the responsible mechanisms for the formation of hydrides, the surface microstructure was further observed and analysed using SEM and EDX, respectively. Around the cuboid particles another phase (seems corrosion stain) was observed (Fig. 11(a)). EDX point analysis on this corrosion stain shows that the contents of O and Mg are high, indicating that this phase may correspond to MgO or $Mg(OH)_2$. TEM's further investigations demonstrate that this phase is $Mg(OH)_2$ (Fig. 12). This result is in agreement with the previous result obtained by synchrotron radiation [22]. Table 1 lists the EDX analysis results for the point A and point B shown in Fig. 12. Point A is on the stain and point B is on the cuboid phase. It is found that at point A both the contents of Mg and O are high. At point B only the content of Dy is very high.

Table 1
Compositions at points A and B shown in Fig. 12.

	Mg	Dy	O
Point A (at.%)	48.3	1.3	50.4
Point B (at.%)	28.0	72.0	0

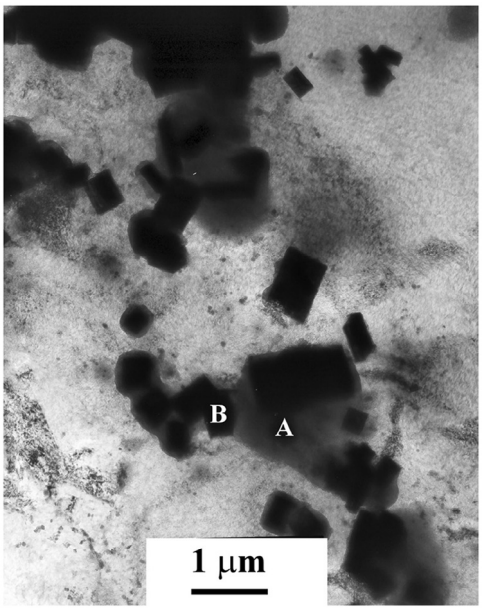

Fig. 12. Morphologies of hydrides in Mg–20Dy alloy with T6 treatment. At points A and B EDX analysis was carried out.

Based on the above results and the present sample preparation processes, the formation mechanism of DyH_2 can be explained as follows:

Firstly, magnesium reacts with water to produce hydrogen:

$$Mg + 2H_2O \rightarrow Mg(OH)_2 + 2[H] \quad (1)$$

Secondly, the produced hydrogen reacts with Dy to form DyH_2:

$$Dy + 2[H] \rightarrow DyH_2 \quad (2)$$

At room temperature, the free energy of $Mg(OH)_2$ is −934.5 kJ/mol and MgO is −609.3 kJ/mol [23]. Hence, $Mg(OH)_2$ would preferably be formed. These observed DyH_2 particles should exist on the surface of samples. In fact, they are caused by the surface reactions when the samples were ground and polished with water. This is why the observed DyH_2 particles always lie on the surface.

The present mechanism for the formation of hydrides in RE-containing magnesium alloys is inconsistent with that proposed by Yang et al. and Zhu et al. [11,13]. Yang et al. identified the formation of hydride NdH_2 in the solution treated Mg–Nd binary alloys [11]. In their investigation, the interesting result is that they found almost the same amount of NdH_2 in Mg–Nd alloy solution treated in air and vacuum. In the as-cast Mg–Nd alloy, no NdH_2 was detected. Therefore, they proposed that the formation of hydride NdH_2 occurred during annealing treatment by the reaction of previously existed hydrogen with Nd. This mechanism is questionable. In fact, the peak with a low intensity (at 28°) corresponding to the NdH_2 exists for the as-cast Mg–Nd alloy which was questioned by Yang et al. (Fig. 2 in Yang et al.'s paper) [11], indicating the possible existence of NdH_2 in the as-cast sample. Unfortunately, they regarded this peak caused by an unknown phase rather than by NdH_2. In checking their observed phenomena and related results in their paper, indeed, it is also shown that the formation of NdH_2 could be explained by the present proposed mechanisms, i.e. by the interaction of solid solute Nd with water or water vapour during their sample preparation. The supported evidence includes: first, in their paper, they did not mention how to prepare their sample, with or without the use of water? Second, their results also demonstrate that the increment in the content of solid solute Nd increases the amount of NdH_2; third, their results also seem to support that the H-agent did not come from the previously dissolved hydrogen in the ingot, if the hydrogen previously existed in ingots it could be escaped during vacuuming and solution treatment, at such a high temperature (813 K) the solubility of hydrogen in Mg is very low; fourth, their samples were water quenched after solution treatment, the samples were touched with water.

In addition, the previous experimental and theoretical investigations show that the solubility of hydrogen is in the range of 20–50 ppm in solid and liquid magnesium or magnesium alloys [24,25]. If such little hydrogen previously existed in the ingot, the amount of hydride formed after the subsequent heat treatment should also be very small, for which it is impossible for XRD to identify. Normally, the critical amount of the second phase detected by XRD is about of 1%–2 wt.%. In Yang's investigation [11], they used XRD to detect the NdH_2, indicating the amount of NdH_2 is not so less. This further concludes that hydrogen may come from the external H-containing agents rather than the previously existed one in ingot.

In Zhu et al.'s investigation [13], they proposed another mechanism that the formation of hydrides is attributed to the decomposition of Mg–RE intermetallics with hydrogen interaction. Although the present results cannot completely exclude their proposed mechanism, it is still demonstrated that their mechanism is also controversial. More investigations are needed in the future to clarify this controversy. Likewise, in Zhu et al.'s paper they did not point out how to prepare their samples, with water machined or not? Their mechanism also cannot explain the formation of hydrides in Mg–RE alloys with T4 treatment in which no Mg–RE intermetallic phases exist. Additionally, as aforementioned, the content of previously existed hydrogen is very low. Moreover, an interesting evidence is that Zheng et al. found the formation of GdH_2 in the solution treated Mg–11Gd–2Nd–0.5Zr alloy, but no NdH_2 was observed although the light RE Nd exists in this alloy [26]. As shown by Mg–Gd and Mg–Nd phase diagrams [14], after solution treatment the solubility of Gd becomes large and its intermetallic phases disappear. In contrast, Nd-containing intermetallics are almost insoluble and they remained after solution treatment because Nd has a very small solubility in Mg matrix. The solubility of Nd in magnesium keeps almost the same. According to the above discussion, the increment of Gd in solid solution after T4 treatment is beneficial for the formation of GdH_2. While Nd still has a low solid solubility after T4 treatment, the formation of its hydride is difficult. Moreover, the absence of NdH_2 demonstrates that the decomposition of Nd-containing intermetallics by hydrogen did not happen. If it had happened, the existence of NdH_2 would have been identified.

4.2. Effect of RE contents

Regarding the influences of RE content on the amount of hydrides, the same results can be obtained in Mg–Y system. Fig. 13 show the effects of Y contents on the formation of YH_2 in Mg–Y alloys. With the increment in Y content, the amount of YH_2 also increases. This further confirmed that the higher the solid solubility of RE in Mg the higher the amount of hydrides. All obtained results in the present investigation concluded that the part of RE in solid solution plays an important role in influencing the formation of hydrides. When the composition of primary alloying element RE increases, its solid solubility in Mg matrix also increases, resulting in the increment of hydride amount.

In order to further confirm the role of RE in the formation of REH_2, a hydrogenation treatment was performed in the present investigation. Fig. 14 shows XRD patterns of hydrogen charged Mg–10Gd samples with T4 treatment. After T4 treatment, the intermetallics formed during solidification dissolved. During the subsequent hydrogenation treatment at 520 °C, which is the same as the solid solution annealing temperature, the dissolved intermetallics cannot be re-formed. The alloying element Gd should mainly exist in Mg matrix with solid solution at such a high temperature. As shown in Fig. 14, in contrast to the previous results, on the sample with dry machined the hydride was still detected. During hydrogenation, the external hydrogen from charging atmosphere could react with Gd in matrix to form the hydrides. After their formation, alloying element Gd was consumed and the content of that part Gd in solid solution reduced. This result in the fact that even the sample with hydrogen charged was machined with water cleaning the amount of hydrides keeps almost the same. Anyway, all these results indicate that Gd with solid solution plays an important role in the formation of hydrides both during sample preparation (with water contacted) and during hydrogenation.

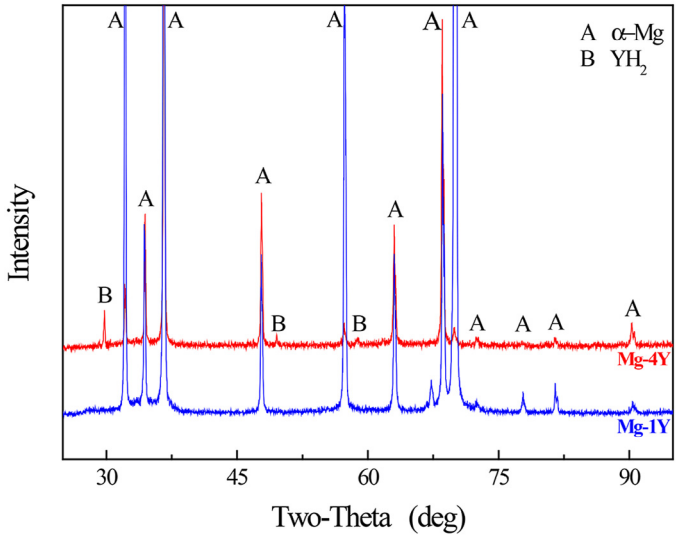

Fig. 13. XRD patterns showing effects of Y content on the formation of YH_2 in Mg–Y alloys with T4 treatment. The samples were prepared with water cleaning.

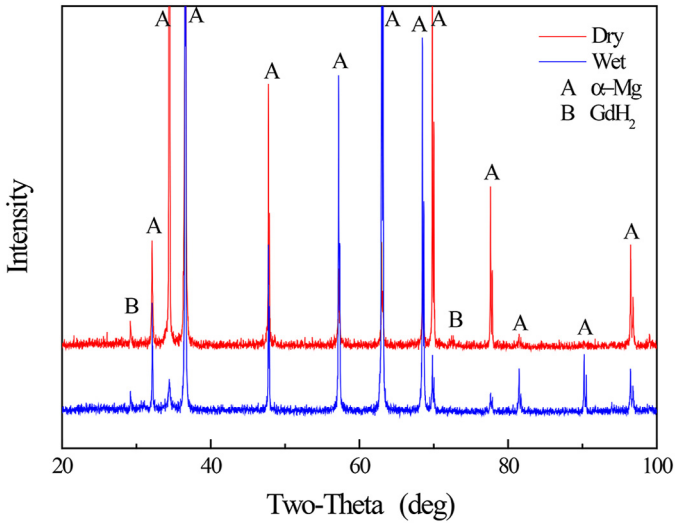

Fig. 14. XRD patterns of Mg–10Gd alloys with hydrogen charged. The samples were prepared by dry and wet machining, respectively. Before hydrogenation, the samples were performed with T4 treatment.

4.3. Effects of heat treatment

The results indicate that the part of Dy which goes into solution in Mg matrix plays an important role in influencing the formation of hydride DyH_2. For the as-cast Mg–20Dy alloy, during solidification the intermetallic $Mg_{24}Dy_5$ is precipitated. A quite part of Dy was used to form this intermetallic. Consequently, the amount of part of Dy to form the hydride DyH_2 reduces, leading to the small amount of DyH_2 on the surface. After Mg–20Dy alloy was T6-treated, the formation of strengthening phase β' consumed most of Dy in Mg matrix [17]. Therefore, the amount of formed DyH_2 on the surface of Mg–20Dy alloy with T6 treatment is small.

Similar to Mg–Dy alloys, after T4 solution treatment the amount of formed hydride YH_2 increases in Mg–4Y alloy (Fig. 15). In this alloy, the content of Y is only 4 wt.%.

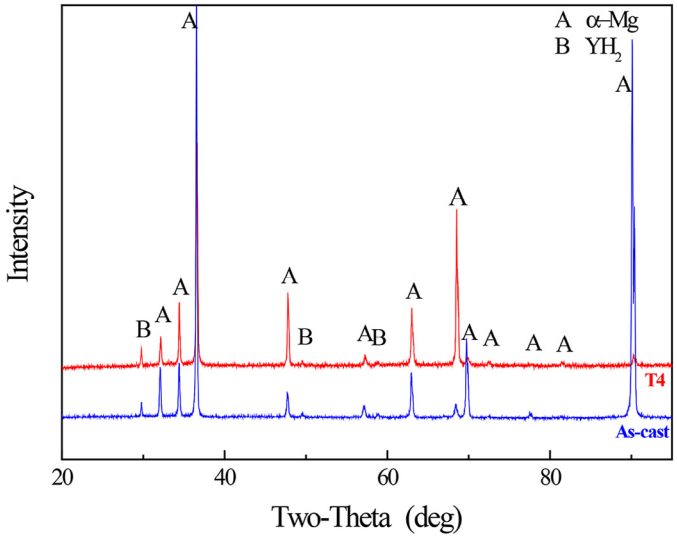

Fig. 15. XRD patterns of Mg–4Y alloys with different sample states.

According to binary Mg–Y phase diagram, at such a content of Y, the amount of Mg–Y intermetallics is quite low. That means even if T4 treatment was carried out and the previously existed Mg–Y intermetallics dissolved, the content of Y with solid solution in matrix changed very small. Consequently, although the amount of YH_2 increases its increment is limited after T4 treatment. That also further supported the conclusion that the formation of hydrides on the surfaces of RE-containing magnesium alloys largely depends on that part of RE with solid solution in Mg.

5. Conclusions

- After Mg–RE (Dy, Gd, Y) alloys are mechanically polished with contact to water, the hydride REH_2 is formed on their surface. Its formation mechanism is attributed to the surface reaction of Mg–RE alloys with water. The part of RE which goes into solid solution in Mg matrix plays an important role in influencing the formation of hydride REH_2.
- The content of RE (Dy, Gd, Y) affects the formation of hydride REH_2 on the surface of Mg–RE alloys. With the increment of RE content the amount of formed REH_2 increases.
- The process of heat treatment influences the formation of hydride REH_2. On the surface of the alloy with T4 treatment the amount of formed hydride REH_2 is higher. In contrast, the amount of REH_2 is low on the surfaces of as-cast and T6-treated Mg–RE alloys.

Acknowledgements

The authors would like to thank Mr. Günter Meister for his technical assistance. They also thank Prof. Florian Pyczak and Mr. Uwe Lorenz for the provision of access to the TEM facilities at Helmholtz-Zentrum Geesthacht.

References

[1] S. Tekumalla, S. Seetharaman, A. Almajid, M. Gupta, Metals (Basel) 5 (2015) 1–39.
[2] N. Birbilis, M.A. Easton, A.D. Sudholz, S.M. Zhu, M.A. Gibson, Corros. Sci. 51 (2009) 683–689.
[3] W. Liu, F. Cao, L. Chang, Z. Zhang, J. Zhang, Corros. Sci. 51 (2009) 1334–1343.
[4] T.J. Luo, Y.S. Yang, Y.J. Li, X.G. Dong, Electrochim. Acta 54 (2009) 6433–6437.
[5] F. Feyerabend, J. Fischer, J. Holtz, F. Witte, R. Willumeit, H. Drücker, et al., Acta Biomater. 6 (2010) 1834–1842.
[6] F. Witte, Acta Biomater. 6 (2010) 1680–1692.
[7] F. Witte, N. Hort, C. Vogt, S. Cohen, K.U. Kainer, R. Willumeit, et al., Curr. Opin. Solid State Mater. Sci. 12 (2008) 63–72.
[8] A.C. Hänzi, P. Gunde, M. Schinhammer, P.J. Uggowitzer, Acta Biomater. 5 (2009) 162–171.
[9] N. Hort, Y. Huang, D. Fechner, M. Störmer, C. Blawert, F. Witte, et al., Acta Biomater. 6 (2010) 1714–1725.
[10] M. Enomoto, Y. Ohata, H. Uchida, J. Alloys Compd. 580 (Suppl. 1) (2013) S3–S5.
[11] Y. Yang, L. Peng, P. Fu, B. Hu, W. Ding, J. Alloys Compd. 485 (2009) 245–248.
[12] Q. Peng, Y. Huang, J. Meng, Y. Li, K.U. Kainer, Intermetallics (Barking) 19 (2011) 382–389.
[13] S.M. Zhu, J.F. Nie, M.A. Gibson, M.A. Easton, Scr. Mater. 77 (2014) 21–24.
[14] A.A. Nayeb-Hashemi, J.B. Clark, Phase Diagram of Binary Magnesium Alloys, ASM International, Metal Park, OH, 1988.
[15] Q. Peng, Y. Huang, L. Zhou, N. Hort, K.U. Kainer, Biomaterials 31 (2010) 398–403.
[16] N. Hort, Y. Huang, D. Fechner, M. Stormer, C. Blawert, F. Witte, et al., Acta Biomater. 6 (2010) 1714–1725.
[17] L. Yang, Y. Huang, F. Feyerabend, R. Willumeit, K.U. Kainer, N. Hort, J. Mech. Behav. Biomed. Mater. 13 (2012) 36–44.
[18] L. Yang, Y. Huang, Q. Peng, F. Feyerabend, K.U. Kainer, R. Willumeit, et al., Mater. Sci. Eng. B Solid State Mater. Adv. Technol. 176 (2011) 1827–1834.
[19] J.D. Verhoeven, A.J. Bevolo, D.T. Peterson, H.H. Baker, O.D. McMasters, E.D. Gibson, Metallography 18 (1985) 277–290.
[20] H.K. Smith, A.G. Moldovan, R.S. Craig, W.E. Wallace, S.G. Sankar, J. Solid State Chem. 32 (1980) 239–243.
[21] H. Oesterreicher, H. Bittner, K. Shuler, J. Solid State Chem. 29 (1979) 191–193.
[22] W. Gan, Y. Huang, L. Yang, K.U. Kainer, M. Jiang, H.-G. Brokmeier, et al., J. Appl. Crystallogr. 45 (2012) 17–21.
[23] I. Barin, Thermochemical Data of Pure Substances: La-Zr, VCH, Weinheim, New York, Basel, Cambridge, Tokyo, 1993.
[24] S.Y. Xu, A.P. Ma, Chin. J. Nonferrous Metals 20 (2010) 628–631.
[25] Z.D. Popovic, G.R. Piercy, Metall. Mater. Trans. A 6 (1975) 1915–1917.
[26] K.Y. Zheng, J. Dong, X.Q. Zeng, W.J. Ding, Mater. Sci. Technol. 24 (2008) 320–326.